# Development of α+β-type biomedical Ti–Nb alloys with high oxygen content

K. Ueda[a,*], M. Omiya[a], Y. Hirose[a], T. Narushima[a]

[a] Department of Materials Processing, Tohoku University, Sendai, Japan

* ueda@material.tohoku.ac.jp

## Abstract

Ti-(5–20)Nb-(0.5–1)O alloys (mass%) were investigated for developing low-cost biomedical α+β-type Ti alloy. Ti-(5, 10, 15, 20)Nb-(0.5, 0.75, 1)O alloys (mass%) were arc-melted and forged into bars. The forged alloy bars were heat-treated at 873 to 1373 K for 3.6 ks in an Ar atmosphere and quenched in iced water. β transus ($T_\beta$) of the Ti-Nb-O alloys decreased with increasing Nb content. An increase in the oxygen content led to an increase in $T_\beta$. After quenching, the formation of α' martensite was observed in Ti-5Nb-*y*O alloys. An increase in the Nb content to 10 mass% led to the formation of α' and α" martensites. A further increase in the Nb content to 15 and 20mass% resulted in the formation of more α" martensites. The boundary temperature for the formation of α' and α" martensite in the Ti-10Nb-*y*O alloys increased with increasing oxygen content, because oxygen enhances the Nb distribution to the β phase. The ultimate tensile strength of the Ti-*x*Nb-0.75O alloys heat-treated to obtain the α-phase fraction ($f_\alpha$) of 0.5 was over 1000 MPa, except for the Ti-15Nb-0.75O alloy. The total elongation decreased with increasing Nb content. The Ti-5Nb-0.75O alloy exhibited excellent strength-ductility balance as a low-cost α+β-type biomedical Ti alloy.

## 1. Introduction

Ti and its alloys have several applications, such as artificial joints, bone plates, and dental implants, as biomedical materials because of their excellent corrosion resistance, mechanical properties, and biocompatibility.[1] Ti-6Al-4V is the most commercially available α+β-type Ti alloy for use in not only biomedical devices but also many fields, such as aerospace components and chemical plants. The α+β-type Ti alloys exhibit a wide range of mechanical properties, which are achieved by the tailoring of volume fraction and grain size of the equiaxed α phase through thermomechanical processing.[2]

It is well known that the production cost of Ti and its alloys is high, and the utilization of ubiquitous elements has been suggested as an effective method of cost reduction for Ti alloys.[3] Oxygen, a ubiquitous element and the main impurity in a Ti sponge, has a high chemical affinity with Ti; this makes purification of the metal difficult.[4] Therefore, utilizing oxygen as an alloying element lowers the production cost of Ti alloys as low-grade Ti sponge and Ti scrap can be employed as raw materials.

The α-phase stabilizability of oxygen is thought to be 10 times larger than that of Al.[5] Studies have reported that the presence of oxygen in Ti increases the hardness and tensile strength of the material but decreases the material's ductility and fracture toughness.[6–8] In our previous study, we focused on V as a β stabilizer in Ti-O alloy systems. [9,10] V is also a β-isomorphous-type element and does not form any intermetallic compounds with Ti. Our previous work investigated the microstructure and mechanical properties of α+β-type Ti-(0–10)V-(0.5–1)O alloys (mass%) using oxygen as an alloying element.[9] Among them, the Ti-4V-0.6O alloy (mass%) exhibited an excellent strength–ductility balance without the formation of athermal ω. In addition, the tensile strength and total elongation of the alloy were comparable to those of the Ti-6Al-4V alloy, indicating good candidature of low-cost α+β-type Ti alloys.

In this study, we also focused on Nb as an alloying element of low-cost biomedical α+β-type Ti alloy. Nb is a β stabilizer and β-isomorphous element with high oxygen solubility. It is also used as an alloying element for biomedical β type Ti alloys. In this study, to develop biomedical α+β-type Ti-Nb-O alloys, the effect of Nb and oxygen on the microstructure and mechanical properties was investigated.

## 2. Materials and experiments

### *2.1 Preparation and heat treatment of specimens*

Commercially pure (CP) Ti, (JIS Grade 2, O: 1038 mass ppm) and $TiO_2$ powder were melted using a non-consumable W electrode in an Ar arc melting furnace to fabricate a master Ti-O binary alloy ingot containing 1.6 mass% oxygen. Following this, the master alloy, CP Ti, and Nb plates were arc-melted to fabricate Ti-Nb-O alloys with four Nb levels and three oxygen levels. The oxygen content in the alloy was measured using the inert-gas fusion-infrared (IR) absorption method (ONH836, LECO, MI). The Nb content was measured using inductively coupled plasma-mass spectrometry (ICP-MS, Agilent8800, Agilent Technologies, CA), and the chemical composition of the alloy is shown in Table 1. After the melting, the ingot was subjected to forging in the β region at 1373 K to a φ12 mm bar followed by air cooling to room temperature. Next, the ingot was forged in the α+β region at 1073 K to a φ8 mm bar, and again followed by air cooling to room temperature. During forging, the alloy was reheated to the forging temperature several times. Hereafter, the forged specimen is referred to as the "as-forged alloy." The as-forged alloy was cut into sections (φ8 × 40 mm) and the residual oxide scale was removed through machining. The heat treatments were conducted in an Ar flow atmosphere at 873–1373 K for 3.6 ks, followed by ice-water quenching. Hereafter, the heat-treated specimen is referred to as the "heat-treated alloy."

**Table 1 Chemical composition of Ti-*x*Nb-*y*O alloys used in this study (mass%)**

| Alloys | 5Nb | | 10Nb | | 15Nb | | 20Nb | |
|---|---|---|---|---|---|---|---|---|
| | Nb | O | Nb | O | Nb | O | Nb | O |
| 0.5O | 4.8 | 0.48 | 10.6 | 0.45 | 15.9 | 0.48 | 20.7 | 0.46 |
| 0.75O | 5.0 | 0.69 | 11.0 | 0.70 | 15.7 | 0.77 | 21.7 | 0.75 |
| 1O | 5.0 | 1.02 | 10.8 | 0.99 | 15.4 | 1.01 | 21.0 | 1.03 |

### *2.2 Specimen analysis*

The constituent phases of the heat-treated alloy were identified through X-ray diffraction (XRD, D8 ADVANCE, Bruker AXS K.K., Karlsruhe, Germany). The microstructure was observed through scanning electron microscopy (SEM, VE-7800, Keyence Co., Osaka, Japan) after mirror polishing and etching in a 2 vol% HF + 13 vol% $HNO_3$ + 85 vol% $H_2O$ solution. The volume fraction of the equiaxed α phase ($f_\alpha$) was calculated from five SEM images (×2000) by using image analysis software (ImageJ, NIH).

Further, the microstructure was observed through transmission electron microscopy (TEM, JEM-ARM200F, JEOL Ltd., Tokyo, Japan). The oxygen and Nb contents of the equiaxed α and β phases were determined using a field emission electron probe microanalyzer (FE-EPMA, JXA-8530F, JEOL Ltd., Tokyo, Japan). Measurements were conducted at 10 positions for each phase and the average value and standard deviation were calculated.

The Vickers hardness of the heat-treated alloys was obtained using a Vickers micro-hardness tester (HM-102, Mitsutoyo Co., Kanagawa, Japan) under a 50 gf load. Uniaxial tensile tests were conducted at room temperature by using a universal material testing instrument (RTF-1325, A&D Co. Ltd., Tokyo, Japan). The tensile specimens were machined to a gage diameter and length of 3 and 10 mm, respectively. The strain rate was set to $5.0 \times 10^{-4}$ $s^{-1}$, and the tensile strength, 0.2% proof stress, and total elongation were measured. The tensile tests were conducted on three specimens for each type of heat treatment

## 3. Results and discussion

### *3.1 Microstructures of the alloys*

Figure 1 shows SEM microstructures of the heat-treated Ti-5Nb-0.5O alloy. The black and gray regions in the figure indicate α and β grains, respectively. Equiaxed α grains were observed in the alloys heat treated at 973 to 1173 K but not after heat treatment at 1223 K. Furthermore, the transformed microstructure, which shows acicular morphology, was observed after quenching from 1073

to 1223 K. By using these images, $f_\alpha$ was calculated and the relationship between $f_\alpha$ and the heat-treatment temperature showed an approach curve. Figure 2 shows β transus ($T_\beta$) of Ti-Nb-O alloys obtained from these approach curves. $T_\beta$ of the alloys decreased with increasing Nb content. Moreover, the increase in oxygen content resulted in increasing $T_\beta$ of the alloys. From these results, the equation for calculating $T_\beta$ of Ti-Nb-O alloys (eq. (1)) was derived.

$$T_\beta\,(\mathrm{K}) = 1155 + 232[\mathrm{O}] - 8.4[\mathrm{Nb}] \quad (1)$$

where [O] and [Nb] are the contents of oxygen and Nb in the alloys, respectively. This equation can predict $T_\beta$ of the alloys within ± 15 K of the experimental value.

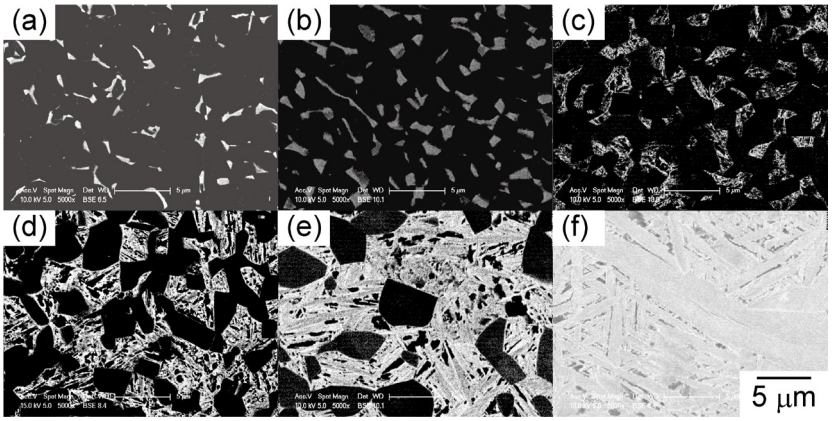


**Fig. 1 Microstructure of the Ti-5Nb-0.5O alloy heat-treated at (a) 973 K, (b) 1023 K, (c) 1073 K, (d) 1123 K, (e) 1173 K, and (f) 1223 K.**

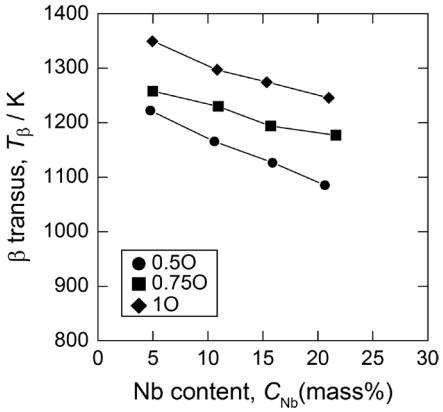


**Fig. 2 $T_\beta$ of the Ti-*x*Nb-*y*O alloys measured through approach curve.**

The constituent phases of the alloys were analyzed through XRD. The formation conditions of the α' and α" martensites in the alloys are summarized in Fig. 3. In the case of the alloys with 0.5-mass% oxygen content (Fig. 3 (a)), the formation of α' martensite was observed in the 5Nb alloy. In the 10Nb alloy, both α' and α" martensites were formed. In the 15Nb and 20Nb alloys, although the formation of α" martensite was detected, α' martensite was not. In the case of the alloys with oxygen content of 0.75 and 1 mass%, the formation of α' and α" martensites were observed in 10Nb alloys, and the boundary temperature for their formation increased with increasing oxygen content. This suggests that Nb distribution to β phase is enhanced by oxygen addition. The distribution of Nb in the α and β phases of the alloys was analyzed through EPMA, and the change in Nb content in the equiaxed α and β phases of Ti-10Nb-0.5O alloy with the change in heat-treatment temperature is shown in Fig. 4. The dashed lines in the figure represent the Nb content of the entire alloy measured through ICP-MS methods. The Nb content in the β phase increased with decreasing heat-treatment temperature, while those of the alloy heat-treated at 1123 and 1073 K were 12.2 and 14.2 mass%, respectively. The α" martensite formed when the Nb content in β phase was reported to be higher than approximately 13 mass%. [11,12] Compared with the α'/α" boundary in the Ti-5Nb-0.5O alloy shown in Fig. 3 (a), the Nb distribution can explain the α'/α" boundary condition, and these results are in good agreement with the Nb content in the β-type Ti alloys.

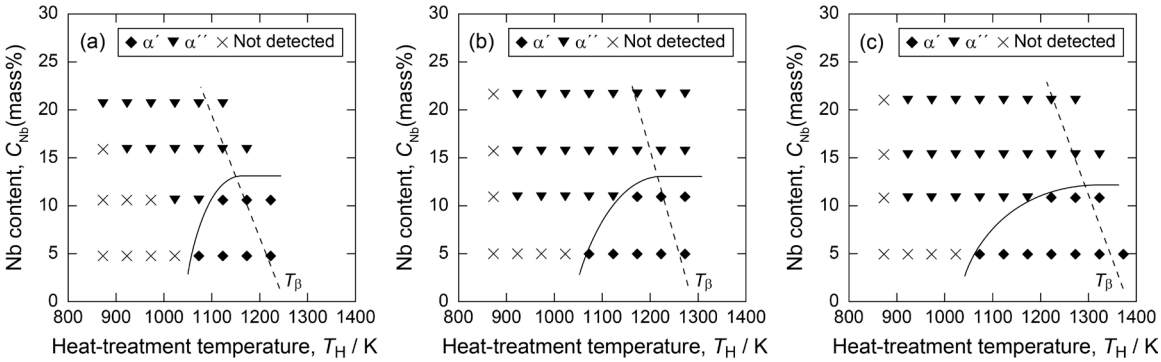


**Fig. 3 α' and α" formation conditions in the Ti-*x*Nb alloys with (a) 0.5, (b) 0.75, and (c) 1 mass% oxygen.**

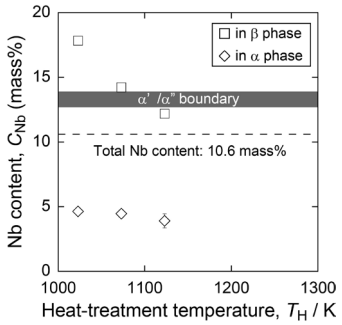


**Fig. 4 Change in Nb contents in the equiaxed α and β phase of Ti-10Nb-0.5O alloy with solution treatment temperature.**

*3.2 Mechanical properties*

Figure 5 shows the change in Vickers hardness of the alloys with change in heat-treatment temperature. In the Ti-10Nb-0.5O and Ti-15Nb-0.5O alloys (Fig. 5 (a)), a significant increase in hardness was observed after heat treatment at 873–973 K and maximum hardness was obtained after heat treatment at 973 K. Under these conditions, athermal ω formed in these alloys after quenching, and its amount was larger in the alloy heat-treated at 973 K. Athermal ω is reported to increase the hardness of Ti alloy. [13,14] Therefore, this study suggests that an increase in hardness of these alloys was caused by the formation of athermal ω. No significant increase in hardness was observed in the alloys with oxygen content of 0.75 and 1 mass%. These results indicate that athermal ω was not formed in the alloys with higher oxygen content because oxygen suppresses the formation of athermal ω. [15]

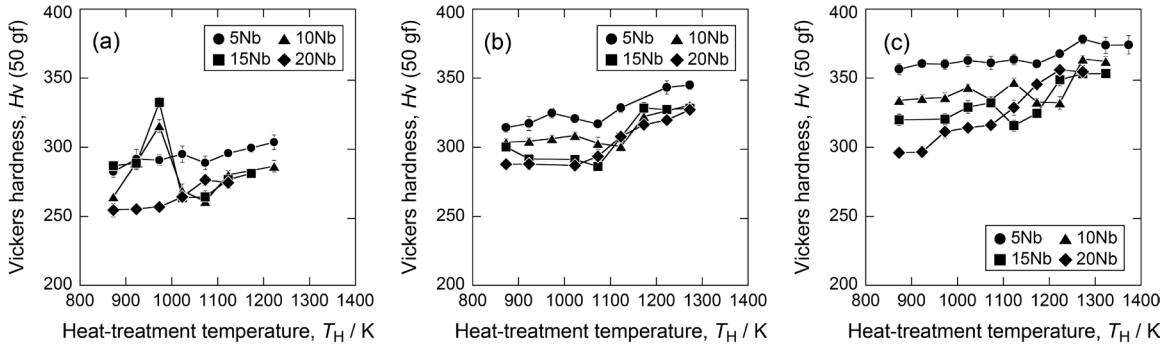


**Fig. 5 Change in Vickers hardness of the heat-treated Ti-*x*Nb-O alloys with heat-treatment temperature. (a) 0.5, (b) 0.75, and (c) 1-mass% oxygen.**

The tensile strength of the alloys with oxygen content of 0.75 mass% was tested and the $f_\alpha$ was fixed to approximately 0.5 by changing the heat-treatment temperatures. The ultimate tensile strength ($\sigma_{UTS}$), 0.2% proof stress ($\sigma_{0.2}$), and total elongation ($L$) of the Ti-*x*Nb-0.75O alloys are shown in Fig. 6. The ultimate tensile strength of the alloys with oxygen content of 0.75 mass% was more than 1000 MPa, except for Ti-15Nb-0.75O alloy heat-treated at 973 K. The total elongation decreased with increasing Nb content. The Ti-5Nb-0.75O alloy exhibited the highest total elongation.

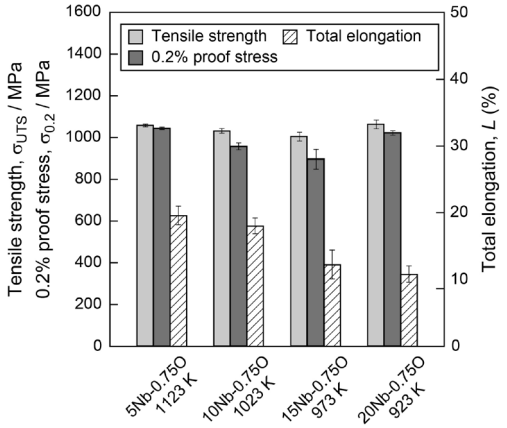


**Fig. 6 Tensile strength, 0.2% proof stress, and total elongation of the Ti-*x*Nb-0.75O alloy, where *x* = 5, 10, 15, and 20.**

A comparison of α+β-type Ti alloys with high oxygen content with other commercially available Ti and Ti alloys [16] is shown in Fig. 7. The figures also shows tensile properties of Ti-4V-0.6O alloy developed in our group.[10] The comparison of the tensile properties of Ti-Nb-0.75O alloys and other Ti alloys shows that the alloy system developed in our group has comparable mechanical properties with those of Ti-6Al-4V alloys. Among Ti-*x*Nb-0.75O alloys, the Ti-5Nb-0.75O alloy exhibits excellent strength–ductility balance as a new low-cost biomedical α+β type-Ti alloy.

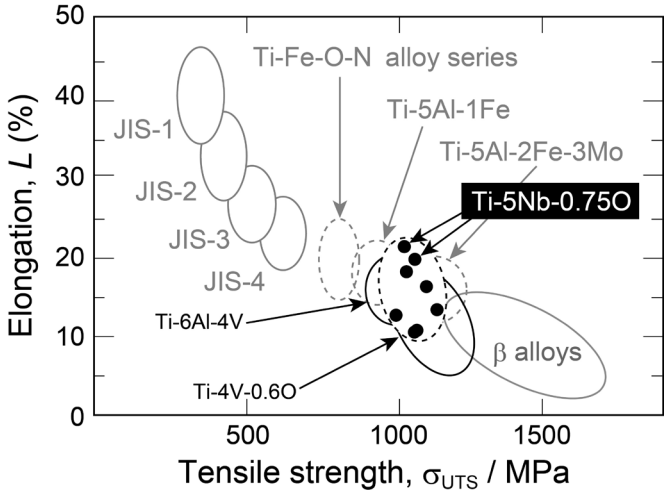


**Fig. 7 Comparison of tensile strength and elongation of the Ti-Nb-O and Ti-4V-0.6O alloys with other commercially available Ti and Ti alloys.**

## 4. Conclusion

The effect of Nb and oxygen on the microstructure and mechanical properties of Ti-Nb-O alloys was investigated, and the following conclusions can be drawn from this study.

- $T_\beta$ of the Ti-Nb-O alloy system was experimentally clarified, and can be calculated as shown in equation (1).
- The formation of α' martensite after quenching was observed in Ti-5Nb-(0.5-1)O alloys. The increase in Nb content to 10mass% led to the formation of α' or α" martensite. A further increase in Nb content to 15 and 20 mass% resulted in the formation of α" martensite.
- The addition of oxygen addition enhanced the distribution coefficient of Nb and enhanced Nb distribution to the β phase, leading to an increase in the boundary temperature for the formation of α' and α" martensites in 10Nb alloys.
- The Ti-5Nb-0.75O alloy exhibits excellent strength–ductility balance.

**Acknowledgments**

The authors would like to thank Dr. Kobayashi of Tohoku University for his TEM analysis. This study was financially supported by a Grant-in-Aid for Scientific Research from the Ministry of Education, Culture, Sports, Science and Technology (MEXT), Japan, under Contract No. 17K06812. It was also supported by the Light Metal Educational Foundation, CRDAM-IMR, Tohoku University, and Creation of Life Innovation Materials for Interdisciplinary and International Researcher Development.

**References**

[1] M. Niinomi, M. Nakai, J. Hieda, Acta Biomater. 11 (2012) 3888–3903.
[2] C. Ouchi, Bull. Jpn. Inst. Mat. 25 (1986) 672–679.
[3] M. Niinomi, J. Jpn. Inst. Met. Mater. 75 (2011) 21–28.
[4] T. Narushima, Titanium Japan 61 (2013) 126–131.
[5] R. Boyer, E.W. Collings, G. Welsch, Materials properties handbook: Titanium alloys, (1994) ASM.
[6] K. Takahashi, E. Sato, Tetsu-to-Hagané 98 (2012) 491–496.
[7] Z. Liu, G. Welsch, Metall. Trans., A, Phys. Metall. Mater. Sci. 19 (1988) 527–542.
[8] T. Hirano, T. Murakami, M. Taira, T. Narushima, C. Ouchi, ISIJ Int. 47 (2007) 745–752.
[9] K. Ueda, T. Kobayashi, T. Narushima, J. Jpn. Inst. Met. Mater. 80 (2015) 60–65.
[10] M. Omiya, K. Ueda, T. Narushima, Mater. Trans. 58 (2017) 1250–1256.
[11] H. Kim, H. Hosoda, S. Miyazaki, J. JILM 55 (2005) 613–617.
[12] D.L. Moffat, D.C. Larbalestier, Metall. Trans. A 19 (1988) 1677–1686.
[13] M. Ikeda, S. Komatsu, J. JILM 55 (2005) 582–586.
[14] E.W. Collings, Physical Metallurgy of Titanium Alloys, (1994) ASM
[15] N.E. Paton, J.C. Williams,Scr. Met. 7 (1973) 647–649.
[16] H. Fujii, K. Fujisawa, M. Ishii, Y. Yamashita, Nippon Steel Technical Report 85 (2001) 107–112.